

SUBSTORM OBSERVATIONS BY SOUNDING ROCKETS AND BY RECEPTION OF POLAR-ORBITTING SATELLITE DATA

T. NAGATA*, T. YOSHINO*, T. HIRASAWA* and H. FUKUNISHI*

Abstract: Comprehensive studies of the polar substorm phenomena could be accomplished by expanding the observation network horizontally by setting arrays of unmanned observatories and vertically by use of balloons, sounding rockets and scientific satellites.

For example of the research coordination between ground-based observatories and sounding rockets, 15 examples of the electron number density profile measured by rockets at Syowa Station in Antarctica are compared with the ground-based observation data. It seems that the auroral ionization by soft precipitating auroral electrons of exp ($-E/2$ keV) in energy spectrum takes place only within auroral arcs, whereas the D-region ionization by hard electrons (>30 keV) is not localized within the auroral arcs.

Satellite data receiving facilities for ISIS-I and -II, INJUN-6, NOAA-III and -IV, ATS-6, EXOS-A and -B have been built at Syowa Station in Antarctica to carry out a continuous observation in coordination with ground-based and rocket-borne measurements. The tracking and receiving capability of the constructed receiving system is represented by preliminary experimental data that over 60 dB of signal-to-noise ratio is maintained above the threshold level for the tracking range over 10^4 km.

1. Introduction

The networks for the observational studies of the substorm phenomena in the earth's polar regions now seem to be widely extended horizontally and vertically for the purpose of simultaneous observations of various elements of the substorm phenomena on ground and in space. In order to fulfil the requirements for the three dimensional extension of substorm observation network, the ground-based network must be supplemented by unmanned ground-based observatories which are to be built up in localities that are important from the observational standpoint but are difficult for mankind to live continuously. Furthermore, the direct measurements of substorm phenomena by means of sounding rockets with a well-established coordination with the simultaneous ground-based observations may give us significant key data to clarify physics of substorms. The balloon-borne measurements of the auroral X-rays, electric field and other associated phenomena also may fall under this category of extended observation system.

* National Institute of Polar Research, 9-10, Kaga 1-chome, Itabashi-ku, Tokyo 173, Japan.

The third category of extended observation networks will be a reception of telemetry signals from the polar-orbiting satellite at the ground-based observatory. As already proved in many satellite experiments, satellite-borne measurements of precipitating particles, electric and magnetic fields, auroras, etc. can supply extremely valuable data for studies of the polar substorm phenomena. If information of these satellite data is directly received at a polar observatory which is a key station of the extended ground-based network including unmanned stations, and at which sounding rockets and balloons are launched, systematic programs for synthetically studying the substorm phenomena can be currently planned *in situ*. Therefore, we planned to carry out this type of synthetic studies of substorm phenomena at Japanese Antarctic station, Syowa, during the IMS period. In this report, some examples of simultaneous observations of Antarctic substorm phenomena obtained by sounding rockets and coordinated ground-based observatories during the period 1970–1973 are summarized. Then, an outline of the receiving system for satellite data in Syowa and results of the preliminary experiments are briefly summarized.

2. Résumé of Sounding Rocket Observations of Ionospheric Electron Density

Up to date, 15 sounding rockets have been launched at Syowa Station (Geomag. lat. = -69.6° , Geomag. long. = 77.1°) to measure the electron number density profile in the southern auroral zone. The apex height of eleven rockets of S-210 type is about 130 km, whereas that of four rockets of S-160 type is about 85 km. In Fig. 1, the electron density profiles thus obtained in nighttime (10 cases in total) and in daytime (five cases in total) are separately summarized. It was practically difficult, however, to shoot a bright auroral arc or band by a sounding rocket even when the auroral activity as a whole is very active and the overhead sky is covered by a number of auroral arcs.

Among 9 time trials to shoot auroral arcs by a S-210 type sounding rocket carrying an electron-probe, only one rocket was able to penetrate a bright auroral arc. All other rockets passed near by or fairly away from bright auroral arcs. Fig. 2 summarized four examples of the electron density profile at nearly the same local time for different degrees of the substorm activity which are represented by the range of negative magnetic substorm (in gammas) and the level of CNA. With an increase of the substorm activity, from -0.3 dB to -4.8 dB in the CNA scale and from -200 γ to -600 γ in the magnetic substorm scale, the electron number density in the lower ionosphere, from 75 km to 100 km in height, increases from 2×10^4 to 4×10^5 electrons/cm³. However, the electron number density in the E-region ionosphere (between 100 km and 130 km in altitude) shows no definite correlation with the auroral electrojet or with the CNA magnitude. This

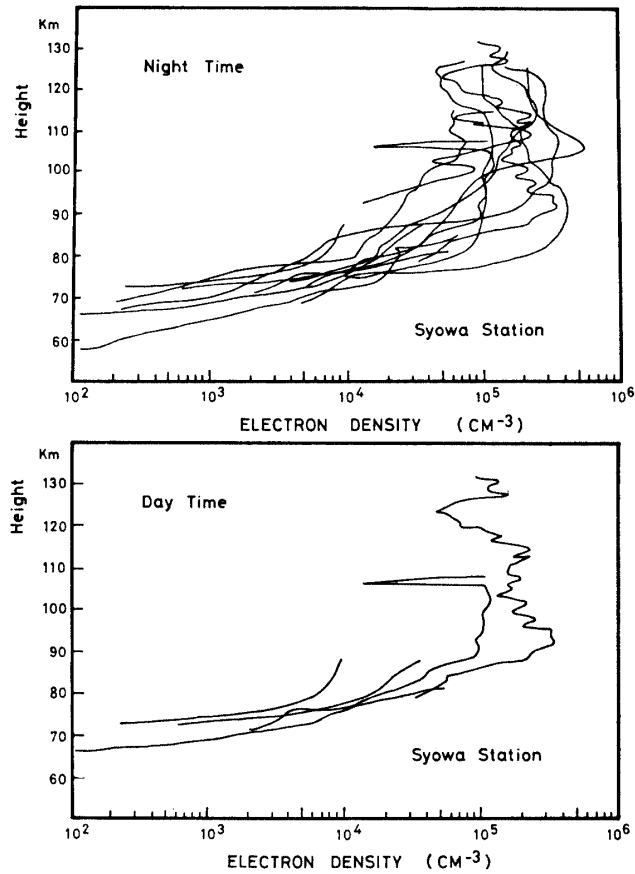


Fig. 1. The vertical profiles of electron density along the flight orbits of sounding rockets during night (up) and day (bottom) hours obtained at Syowa Station in Antarctica.

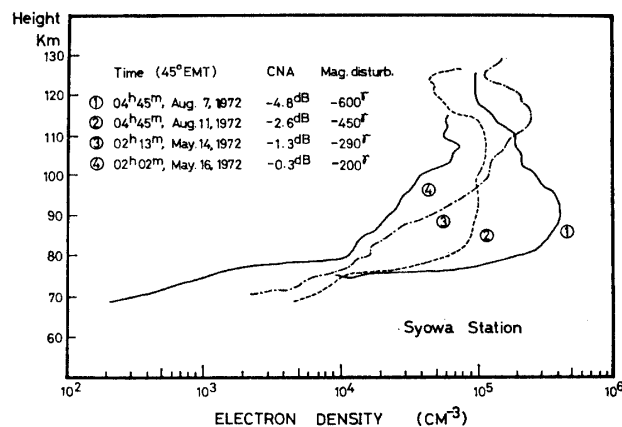


Fig. 2. The vertical profiles of electron density along the flight orbits of sounding rockets, when the polar substorms of various degrees took place at Syowa Station in Antarctica.

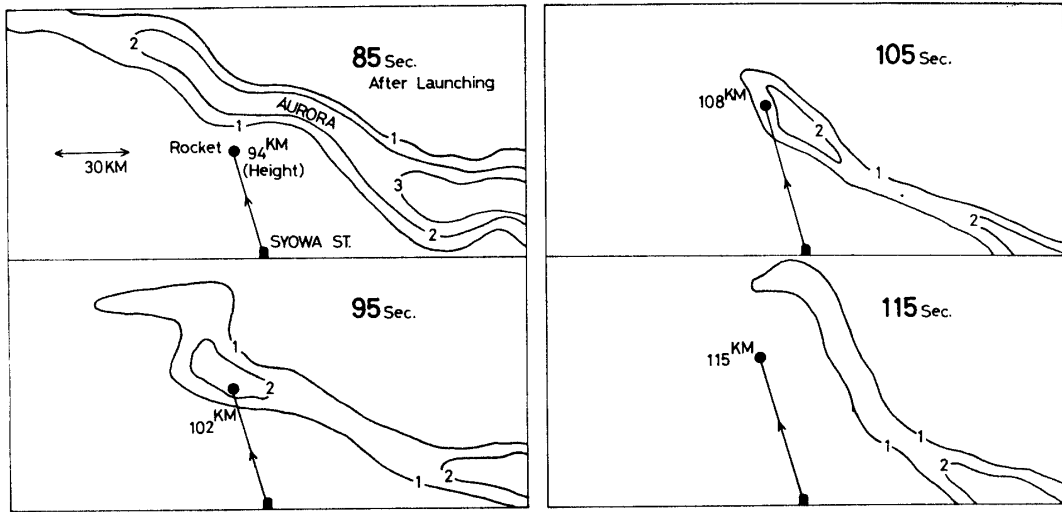


Fig. 3. Horizontal projections of the auroral arc and the position of the ascending rocket 85, 95, 105 and 115 seconds after launching. The numerals of contours represents $N_2+4278 \text{ \AA}$ auroral luminosity in unit of kR .

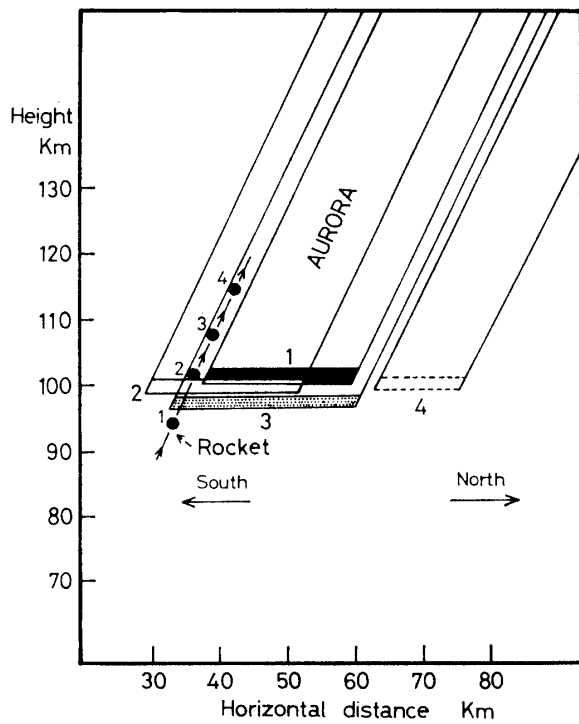


Fig. 4(a). Vertical projections on the geomagnetic meridian plane of the auroral arc and the position of the ascending rocket. 1, 2, 3 and 4 represent respectively times of 85, 95, 105 and 115 seconds after launching the rocket. (00^h54^m GMT. August 23, 1973. Syowa Station, Antarctica)

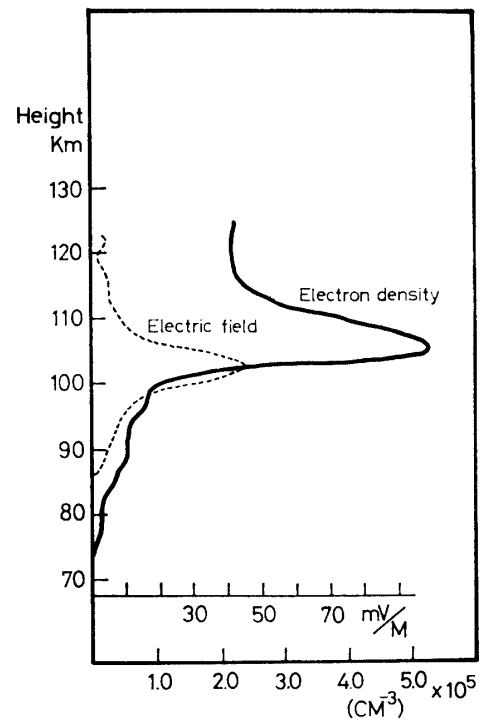


Fig. 4(b). The vertical profiles of the electron density and the horizontal electric field along the flight orbit of a sounding rocket which penetrated into an auroral arc at altitude of about 100–110 km. (00^h54^m GMT. August 23, 1973. Syowa Station, Antarctica)

result may be due to the condition that these rockets did not pass through a bright auroral arc.

When a sounding rocket penetrates an auroral arc, on the contrary, an anomalous local ionization of the E-region ionosphere is observable. With the aid of all-sky camera auroral photographs at intervals of 10 seconds, multi-color scanning auroral photometry data at intervals of 5 seconds for $\text{OI } 5577 \text{ \AA}$ and $\text{N}_2^+ 4278 \text{ \AA}$ and a continuous record of auroral radar observation, a relative position in space of the rocket with respect to the auroral arc can be traced as a function of time. Fig. 3 shows the horizontal projections of the luminosity of $\text{N}_2^+ 4278 \text{ \AA}$ emission of an auroral arc and the flight orbit of an electron-density measuring rocket, S-210JA-18 which was launched at 00^h36^m GMT, August 23, 1973 from Syowa Station, whereas Fig. 4(a) illustrates the projections of the auroral arc and the rocket flight orbit on the geomagnetic meridian plane. As shown in these figures, the rocket penetrated the auroral arc at an altitude of about 100 km about 90 seconds after the launching, but the auroral arc moved away northwards from the rocket flight orbit at about 110 km of the rocket altitude.

The vertical profile of the electron number density along the rocket flight orbit is given in Fig. 4(b), where a large increase of electron density (about 5×10^{-6} electrons/cm³ at maximum) is observed only in an altitude range of 100–110 km. This result may indicate that the electron number density (N) in the E-region markedly increased only within the bright auroral arc and the N value is much reduced at stage 4 in the figures when the bright auroral arc moved away from the rocket flight orbit and only faint diffuse auroras might surround the path of rocket flight.

As the simultaneous scanning observation of H_β luminosity has indicated that no appreciable effect of precipitating protons can be expected in the auroral arc at the times concerned, it is no doubt that the auroral excitation and the ionization in this case were caused by precipitating electrons. Then, combining the electron number density profile and the intensity of $\text{N}_2^+ 4278 \text{ \AA}$ as functions of the rocket flight orbit, the flux and energy spectrum of precipitating electrons can be evaluated reasonably well by assuming that the basic equation of the electron number density (N) at height (z) is expressed by

$$\frac{d}{dt}N(z) = \int_0^\infty f(E)Q(E, z)dE - \alpha_{\text{eff}}N^2, \quad (1)$$

where $f(E)$, $Q(E, z)$ and $\alpha_{\text{eff}}(z)$ denote respectively the energy spectrum of precipitating electrons, the ionization rate for energy E at height z and the effective recombination coefficient of electrons at z (REES, 1963; KAMIYAMA, 1966). In the following, only results of such evaluations of $f(E)$ and the electron flux

(F_0) will be given, techniques in detail of theoretical approach being reported elsewhere (NAGATA *et al.*, 1975); namely, the theoretical analysis has given that

$$f(E) = \frac{1}{2\pi E_0} F_0 \exp(-E/E_0), \quad (2)$$

where $E_0 = 2$ keV,

$F_0 = 9.2 \times 10^9$ electrons/cm²/sec corresponding to $I(4278 \text{ \AA}) = 1$ kR.

The energy spectrum and flux of the precipitating auroral electrons can stand well for the observed electron number density profile and the observed luminosity of $N_2^+ 4278 \text{ \AA}$ in the E-region. An approximate value of α_{eff} also can be estimated by assuming that N in stage (4) in Figs. 3 and 4 represents the electron number density 10 seconds after a stop of the ionization by the precipitating electrons which had resulted in the maximum ionization of $N_0 = 5 \times 10^6$ electrons/cm³, namely by use of relation

$$N = \frac{N_0}{1 + N_0 \alpha_{\text{eff}} t}. \quad (3)$$

$\alpha_{\text{eff}} = 3 \times 10^{-8}$ (electron)⁻¹ (sec)⁻¹ thus empirically obtained is in good agreement with the theoretically estimated value (FUJITAKA *et al.*, 1971).

However, the observed electron number density in the D-region is too large to be attributed to the ionization effect of the precipitating auroral electrons. The substorm activity during the rocket flight given in Figs. 3 and 4 is represented by -0.5 dB in CNA and -50γ in the magnetic substorm range on ground. This substorm activity is therefore nearly the same as or a little smaller than that in case (4) given in Fig. 2. On the other hand, the D-region ionization in all cases of Fig. 2 through Fig. 4 is too large to be attributed to an effect of the aurorally associated Bremsstrahlung X-ray also (REES, 1964; KAMIYAMA, 1970). Then a possible interpretation would be that the spectrum of precipitating electrons is not uniquely represented by a simple exponential law such as expressed by (2), but comprises two components, *i.e.* one is energetically soft and responsible for the ionization and optical excitation in the E-region, and the other is energetically hard and responsible primarily for the ionization in the D-region. To be consistent with the observed non-localized nature of CNA in association with auroras, the hard component (>30 keV) of auroral electrons may have to be spread over an extended area of the substorm region, but not localized within the bright auroral arcs. The soft component, on the other hand, may be localized and confined to bright auroral arcs.

3. Reception of Telemetry Signals from Polar-Orbiting Satellites

As already mentioned in the introduction, a synthetic study of the substorm phenomena by combining satellite data with simultaneous ground-based, rocket

Table 1. Reception program of satellite data at Syowa Station in 1976.

National name	Apo. (km)	Peri. (km)	Inc.	Period (min)	Objectives	Sponsor
ISIS-I	3514	574	88.42°	128.21	Topside sounding VLF etc.	Canada (CRC) -USA (NASA)
ISIS-II	1429	1367	88.16°	113.6	"	"
NOAA-III	1509	1500	102.03°	116.09	Visible, IR	NOAA/NASA
NOAA-IV	1457	1443	101.7°	114.9	"	"
INJUN-6 (Hawkeye)	125570	469	89.8°	3032.4	ELF/VLF etc.	NASA
ATS-6	35700	35700	0°	24 hour	Radio beacon etc.	"

Table 2. Reception program of satellite data at Syowa Station after 1977.

National name	Launch year	Apo. (km)	Peri. (km)	Inc.	Objectives
ISS-II	1/77	1000	1000	70°	Topside sounding
EXOS-A	1/78	4500	300	65°	ELF/VLF
EXOS-B	5/78	29000	250	30°	ELF/VLF

and balloon ones will result in an extreme progress in obtaining the overall physical view of the phenomena. Therefore, we have planned to build up a satellite data telemetry receiving station in Syowa in Antarctica in early 1976. Then, the telemetry signals from ISIS-I, -II, NOAA-III, -IV, INJUN-6 and ATS-6 will be received in 1976. The orbit parameters of these satellites as well as the scientific data objectives are listed in Table 1. The telemetry signals from the Japanese polar-orbiting satellites ISS-II and EXOS-A, -B will be received after 1977. The orbit parameters and the objectives of observations are listed in Table 2.

The antenna tracking and receiving systems for this program have been specifically designed and constructed by Scientific Atlanta Co. with cooperation of one of the authors (T. YOSHINO) in regard to the special requirements on the basis of Antarctic circumstances. The whole system consists of a dual frequency band antenna subsystem, RF tracking electronics, pedestal and servo-control subsystem and receiving subsystem.

For example, the antenna subsystem, shown in Fig. 5, is a special product for the Antarctic use, specifically with respect to a convenient geometry and mechanical structure for the construction and operation by a few wintering members and the necessary protection from the heavy streams of very fine drifting snow particles in Antarctica. This antenna subsystem consists of two independent

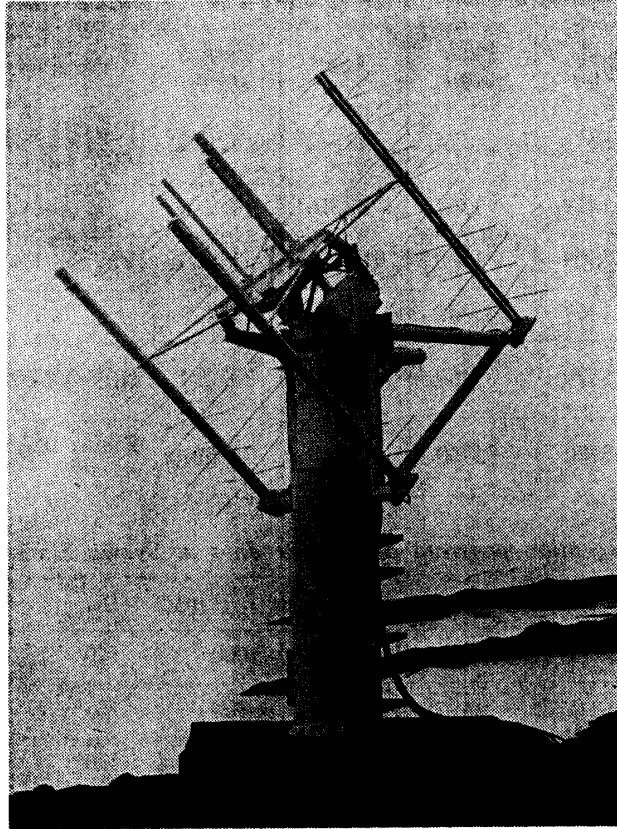


Fig. 5. 136 and 400 MHz dual band log-periodic antenna array system for the satellite telemetry reception at Syowa Station.

sets of 4 stacked 9 element crossed log-periodic array, which are co-located on a common mounting structure. The VHF array has a function of monopulse tracking system operating in the frequency band of 136–138 MHz, whereas the UHF one operates in a receive-only mode in 400 MHz band. The block diagram of this reception system is given in Fig. 6. The appropriate band-pass filtering and preamplification networks are packed into the rear side of the antenna mounting structure for the purpose of safety against the snow storms. Main characteristics of the antenna system as a whole are as follows:

(1) Antenna system

VHF 136 MHz monopulse tracking antenna array.

4 stacked 9 element crossed log-periodic array. Gain 18 dB max.

UHF 400 MHz receive-only antenna array.

4 stacked 9 element crossed log-periodic array. Gain 18 dB max.

(2) Filter/Preamplifier

VHF 136 MHz pre-amplifier.

Gain 26 dB, NF 1.46 dB.

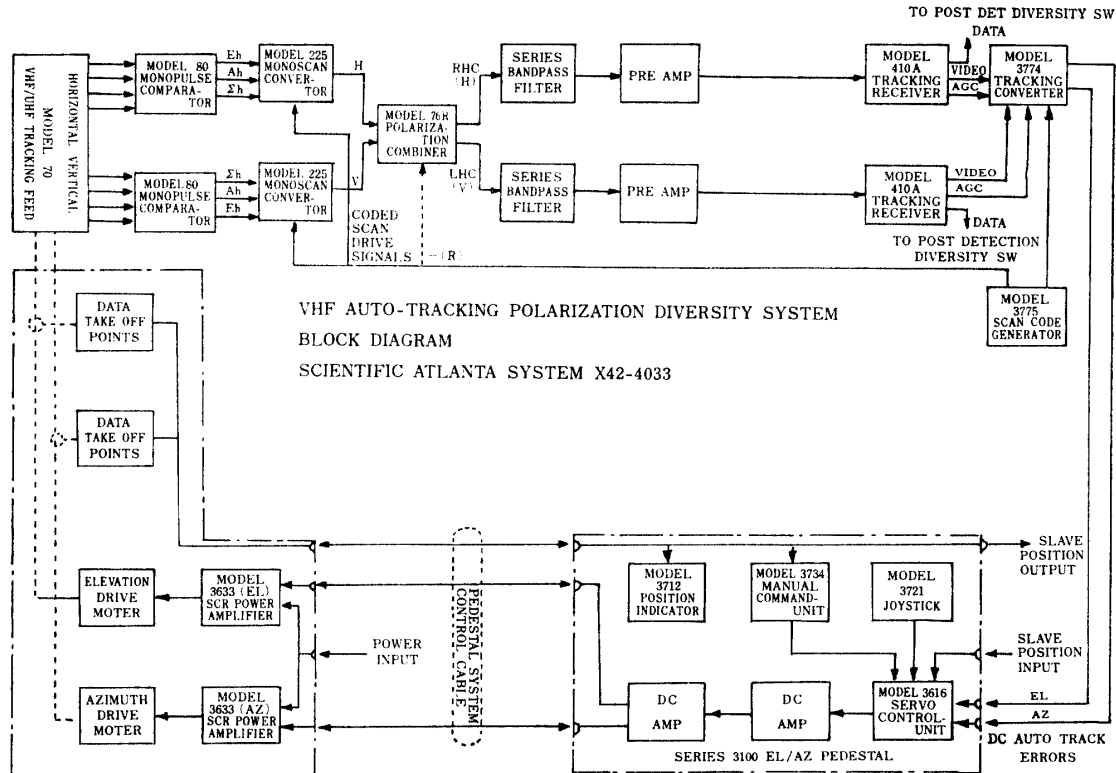


Fig. 6. A block diagram of satellite tracking system.

UHF 400 MHz pre-amplifier.

Gain 24 dB, NF 2.25 dB.

(3) Tracking characteristics

Model 3100 EL-AZ pedestal.

AC servomotor 2 each axis; Delivered torque 1000 lbf-ft.

Pedestal system accuracy less than 0.05° .

Low temperature modification -40°C .

The signal flows from the preamplifier outputs are connected through a long co-axial cable to the receiver system in an observatory hut. The tracking video signal of the tracking receiver is input to the tracking converter. This unit allows the optimum signal selection (RHC and LHC) for both requirements for scientific data and the tracking function. The data channel output is available for the furnished processing and/or recording need. The single channel tracking information is synchronously detected and demodulated to provide the necessary azimuth and elevation error signals for keeping the continuous satellite tracking through the pedestal servo-system. Main characteristics of the tracking and receiving subsystems are summarized in the followings:

(1) Tracking and main data receiver

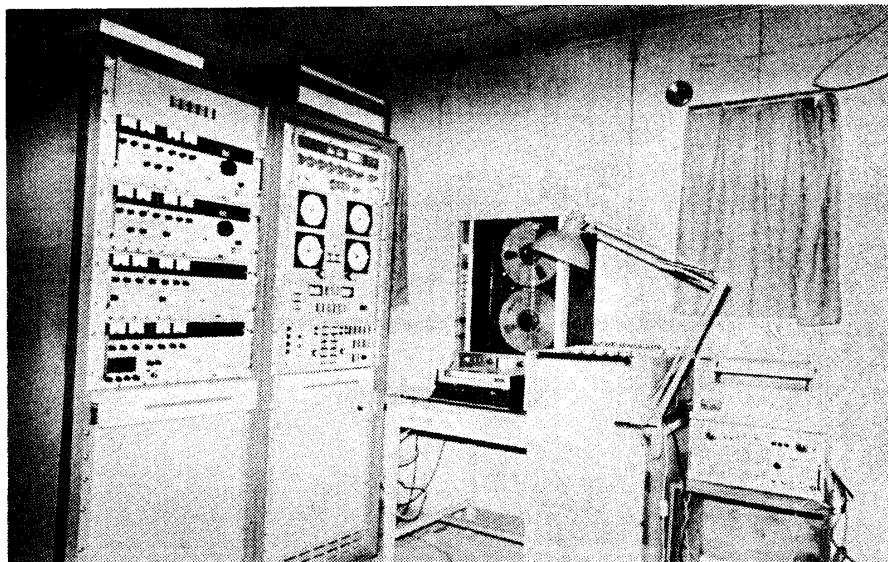


Fig. 7. Receiving system and attached recording and drawing equipments at the Syowa Satellite Earth Station.

- (i) Model 410A basic receiver.
- (ii) Frequency range 136–138 MHz and 395–410 MHz RF tuner.
- (iii) Standard FM demodulator.
Deviation 15 kHz–1.5 MHz.
- (iv) Narrow band FM demodulator.
- (v) FM demodulator.
Deviation: $(\pm 20^\circ) - (\pm 135^\circ)$.
Fine tuning range: ± 250 kHz.
Lock threshold: -20 dB SNR at IF; $+2$ dB in loop.
- (2) Receiver overall characteristics
RF input: 50 ohm–105 dBm (less than $0.1 \mu\text{V}$).
First IF: 60 MHz.
Second IF: 10 MHz.
Video filter linear phase: 18 dB/oct. reel off.
20, 50, 100, 200, 500 kHz and 1 MHz
Video amp.: Output 0–8 Vpp, AC and DC.
Data rate: Up to 5 Mbits.

Fig. 7 illustrates the arrangement of these equipments installed in the upper atmosphere physics laboratory at Syowa Station.

Preliminary experiments of tracking and reception performance by the satellite reception system were carried out in central Japan from July to September 1975. The experiments were performed by the upper atmosphere physics research members only of the Antarctic wintering term, partly for the purpose of

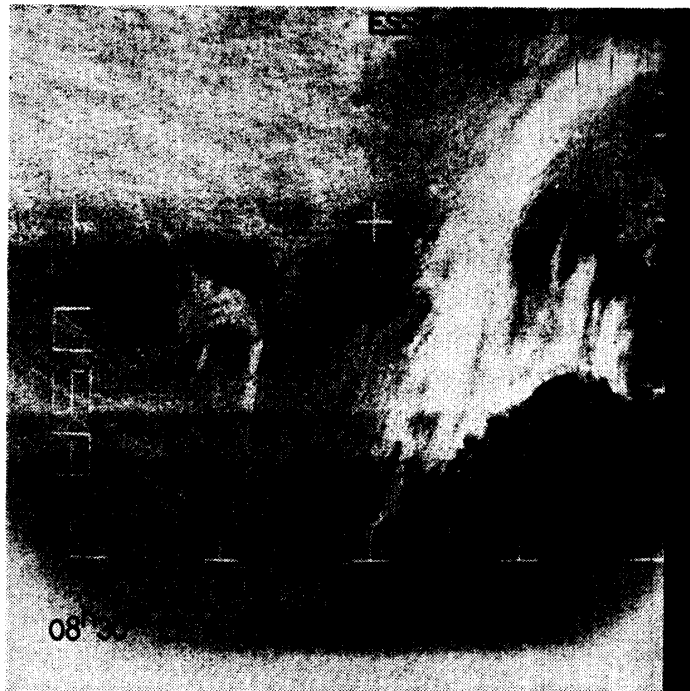


Fig. 8. *An example of ESSA-8 video-camera photograph of Enderby Land area.*

Black parts: clouds and ocean.

White parts: snow-covering continental area (no cloud).



Fig. 9. *An example of NOAA-IV radiometer photograph of Enderby Land area.*

Black parts: clouds and ocean.

White parts: continental area of no cloud.

training of the assembling, construction and maintenance as well as operation of the whole system. The test experiments were made for 7 satellites such as ISIS-I, ISIS-II, ATS-1, TAIYO (a Japanese scientific satellite SRATS), INJUN-6, NOAA-III and NOAA-IV. Results of the test experiments were sufficiently satisfactory. The maximum trackable sensitivity at 136 and 400 MHz frequency band has been represented by the experimental data that over 10 dB in signal-to-noise ratio is maintained above the threshold level for the tracking range exceeding 10,000 km, provided that the boarding transmitter power is 1 watt and the telemeter transmitting antenna gain is 0 dB while the maximum data transmission rate is 5 Mbits.

As shown in Fig. 5, the antenna system has been mounted on a small rock hill at the northeast corner of Syowa Station area, the geographical location of which is $69^{\circ}00'03''\text{S}$ and $39^{\circ}35'06''\text{E}$. The elevation of antenna base is 16 m about the sea level. The observatory shown in Fig. 7 is about 50 m separated from the antenna site. In the preliminary observation at this Syowa Satellite Earth Station (SSES), this new receiving system is currently receiving the signals of over 20 satellites everyday, and in particular, it is receiving those of ISIS-I and -II, NOAA-IV and ESSA-8 on the routine basis. The maximum signal level is 66 dB over the noise level in these routine observations. Figs. 8 and 9 illustrate early examples of the visual signal receptions from ESSA-8 and NOAA-IV respectively.

From April 1, 1976, the receivings of telemetry signals from ISIS-I and -II and NOAA-III and -IV have become routine observation programs at the SSES. The following is a summary of the results of these observations during about one month.

3.1. *ISIS-I and ISIS-II*

The automatic tracking characteristics of the antenna system for ISIS satellites whose transmitting power is 90 mW and whose frequency is 136.410 MHz are satisfactorily good even in bad weather conditions such that atmospheric temperature is -23°C and wind speed is 30 m/sec: namely, the antenna gain is 0 dB; the signal-noise ratio is over 46 dB; the antenna tracking error is less than $\pm 1.2^{\circ}$ for 4,200 km in the satellite distance and 30 kHz in the IF width of the receiving system.

The main research programs by use of the ISIS telemetry data are synthetic studies of the auroral VLF emissions and the polar ionosphere structure in combination with the ground-based observing network and sounding rocket observations. For the elevation angle range of ISIS orbits of 23° – 89° , the received signal-noise ratio for the telemetry signals ranged from 25 dB to 52 dB. A large number of data thus received are supplying almost perfect information about VLF hiss, chorus and whistler emissions and the topside ionograms. For example,

ISIS-II data of strong emissions of VLF hiss were received at the SSES from 20^h37^m to 20^h43^m GMT, April 8, 1976 when the satellite elevation was about 89°, while Syowa Station VLF observatory simultaneously recorded the similar VLF hiss emissions. Planned programs to launch auroral VLF sounding rockets at Syowa Station (such as the S-210JA-20 program) will be able to achieve a genuine three-dimensional study of the auroral VLF emissions, if the launching can be appropriately carried out at the time when ISIS data of VLF emissions and topside ionograms over the head of Syowa Station are available together with ground based ones of optical, radio and magnetic records of the auroral flare phenomena.

3.2. *NOAA-III and NOAA-IV*

The routine work to receive the infra-red radiation data from NOAA-III and NOAA-IV has been continued from April 1, 1976. The routine receiving work has been set twice a day, *i.e.* in the early morning and in the midnight, and the IR remote-sensed area covers almost the whole Antarctic Continent. Those infra-red radiation data are currently supplying clear information about the inflow of warm air-mass into the continent and the outflow of cold air-mass from the continent, which is essentially important in the meteorological research of this area. However, discussions of these meteorological data will be made elsewhere.

4. Concluding Remarks

In this note, the capability and characteristics of the sounding-rocket launching facility and the satellite telemetry signal receiving one at Syowa Station in Antarctica are outlined. Although the maximum altitude of flight orbit of S-210 type sounding rockets is about 130 km, that of S-310JA-1 rocket which was launched on February 14, 1976 reached the maximum height of about 215 km. During the IMS period, both S-210 and S-310 sounding rockets will be launched at Syowa Station for respective research purposes in relation to the auroral flare studies. Then the synthetic observation programs of the polar ionosphere by use of the bottom-side ionosonde, the riometer and the auroral radar on the ground, the electron-probe and the ion-probe in sounding-rockets, and the topside ionograms from ISIS satellites will be able to perform a complete ionosphere measurement.

In regard to the auroral VLF emission studies, the ground-based observation facility at Syowa Station comprises a VLF signal recorder of 22.3 and 17.4 kHz in frequency, a VLF direction finder, a chorus recorder for a continuous frequency band of 0.2–10 kHz, and a narrow-band intensity recorder of 0.75, 1, 2, 4, 5, 8, 12, 14, 28, 32, 50, 64 and 128 kHz in frequency. In addition, Mizuho Camp, which is located about 300 km southeast of Syowa Station, will soon be facilitated with a chorus recorder for 0.2–10 kHz in frequency and a narrow-band intensity

recorder of 0.75, 1, 2, 4, 8 and 28 kHz together with other auroral flare observing equipments. The planned simultaneous observations of auroral VLF emissions with the rocket-borne recorders, the ISIS telemetry signal receiving and these ground-based observations are expected therefore to result in a complete set of data of this problem.

In concluding, the authors wish to express their thanks to Miss M. TAKIZAWA who helped them in analysis of the sounding rocket data, and to Mr. T. MATSUO who assisted them in setting the Syowa Satellite Earth Station in Antarctica.

References

- FUJITAKA, K., T. OGAWA and T. TOHMATSU (1971): A numerical computation of the ionization redistribution effect of the wind in the night-time ionosphere. *J. Atmos. Terr. Phys.*, **33**, 687–700.
- KAMIYAMA, H. (1966): Ionization and excitation by precipitating electrons. *Rep. Ionos. Space Res. Japan*, **20**, 171–187.
- KAMIYAMA, H. (1970): Ionization effect of the Bremsstrahlung associated with precipitating electrons. *Ann. Geophys.*, **26**, 625–630.
- REES, M. H. (1963): Auroral ionization and excitation by incident energetic electrons. *Planet. Space Sci.*, **11**, 1209–1218.
- REES, M. H. (1964): Ionization in the earth's atmosphere by aurorally associated Bremsstrahlung X-rays. *Planet. Space Sci.*, **12**, 1093–1108.
- NAGATA, T., T. HIRASAWA, M. TAKIZAWA and T. TOHMATSU (1975): Antarctic substorm events observed by sounding rockets; Ionization of the D- and E-regions by auroral electrons. *Planet. Space Sci.*, **23**, 1321–1327.